


Extinction transition of hantavirus-infected rodents in a hostile environmentChing-Jung Chen, Yuan-Zhang Gu, and Kuo-An Wu^{*}*Department of Physics, National Tsing Hua University, Hsinchu 30013, Taiwan* (Received 21 May 2021; revised 2 August 2021; accepted 20 October 2021; published 8 November 2021)

The spatial critical shelter sizes above which populations would survive are investigated for the infection of hantavirus among rodent populations surrounded by a deadly environment. We show that the critical shelter sizes for the infected population and the susceptible population are different due to symmetry breaking in the reproduction and the transmission processes. Therefore, there exists a shelter size gap within which the infected population becomes extinct while only the susceptible population survives. With the field data reported in the literature, we estimate that, if one confines the rodent population within a stripe region surrounded by a deadly environment with the shorter dimension between 335.5 ± 27.2 m and 547.9 ± 78.3 m, the infected population would become extinct. In addition, we introduce two factors that influence the movement of rodents, namely, the spatial asymmetry of the landscape and the sociality of rodents, to study their effects on the shelter size gap. The effects on the critical size due to environmental bias are twofold: it enhances the overall competition among rodents which increases the critical size, but on the other hand it promotes the spread of the hantavirus which reduces the critical size for the infected population. On the contrary, the sociality of rodents gives rise to a more localized population profile which promotes the spread of the hantavirus and reduces the shelter size gap. The results shed light on a possible strategy of eliminating hantavirus while preserving the integrity of food webs in ecosystems.

DOI: [10.1103/PhysRevE.104.054401](https://doi.org/10.1103/PhysRevE.104.054401)**I. INTRODUCTION**

Hantavirus pulmonary syndrome (HPS) is a severe and potentially life-threatening respiratory disease [1,2]. The specific species of hantavirus named Sin Nombre virus [3], which causes the disease, is transmitted to humans from infected rodents through contact with rodents' saliva, urine, and droppings. HPS has attracted much attention since its first known outbreak in the Four Corners region of the southwestern U.S. in 1993, and in this case, the hantavirus is found to be carried by *Peromyscus maniculatus*, the deer mouse [4]. In contrast to its deadly threat to humans, infected rodents show no signs of illness and the susceptible rodents could get infected through physical contact with infected rodents [5–7]. Since the contraction of the disease closely depends on rodent activities, the spatiotemporal distribution of rodent populations is important to understand the spatial spread of the hantavirus.

By considering principal ingredients for the evolution of the rodent population based on biological observations, such as birth, death, competition for resources, movement, and the horizontal transmission of the virus among them, Abramson and Kenkre proposed a theoretical model to study the spatiotemporal patterns of the rodent population [8]. With this phenomenological model, it is shown that the survival or extinction of the infected population is strongly correlated to the spatiotemporal distribution of the carrying capacity of the environment [8–11], which is consistent with reported observations [2,6,7,12]. A critical carrying capacity is iden-

tified in the study, below which the infected population would become extinct unless a resource-rich environment is nearby. Due to its success, further generalizations of the model are made to include the Allee effect [13–16] which addresses a possible survival fitness change with the population [17,18], the age-group-dependent mobility [19,20], time-delay effects due to maternal antibodies for juvenile rodents [21,22], etc. Nonetheless, the carrying capacity is shown to play a crucial role in the survival or extinction of the infected population. In this paper, we show that, even if the carrying capacity is above the critical value, the infected population could become extinct and only the susceptible population survives in a shelter surrounded by a hazard environment.

The theoretical study of a critical patch size for the population to survive as it is surrounded by a deadly environment was first carried out by Kierstead, Slobodkin, and Skellam (KiSS) in the 1950s [23,24]. The critical patch size, which is named the KiSS size, is the minimal spatial patch size below which the population becomes extinct regardless of the abundance of resources within the patch. This characteristic length scale is associated with the competition between the reproduction of the population in the bulk volume and mortality of the population on the surface due to diffusion [25]. The KiSS size is extensively studied theoretically [23,25–30], and it has been applied to a wide range of ecological systems such as bacteria [31–36], plankton [24,37], and birds [38–40].

In this study, we investigate how the shelter size impacts the survival of the hantavirus-infected and the susceptible rodents surrounded by a hazardous environment. We show analytically and numerically that there exists two KiSS sizes, one for the infected population and one for the susceptible

^{*}kuoan@phys.nthu.edu.tw

population, between which the infected population becomes extinct and the susceptible population survives. It sheds light on a possible strategy for eliminating hantavirus while preserving the integrity of food webs in ecosystems. In addition, we explore how two common factors, namely, the bias of the movement due to the landscape such as the mountain slope and the social nature of rodents, affect the shelter size gap. We find that the environmental bias results in asymmetric population profiles which give rise to an overall keener competition between rodents. Therefore, an increase in the critical size is expected if the competition is solely considered. However, the asymmetric population profile could promote the spread of the hantavirus due to the densely packed region of the asymmetric population profile, which would reduce the critical size for the infected population. On the other hand, sociality of rodents would drive the population to be more localized that promotes the spread of the hantavirus. Therefore, the shelter size gap is shown to shrink as expected.

This paper is organized as follows: In Sec. II, we briefly review the population model for the spatial spread of the hantavirus by Abramson and Kenkre. In Sec. III, the KiSS sizes for the infected population and susceptible population are obtained analytically using a Galerkin truncation method (GTM) [41], and the results are in good agreement with numerical simulations quantitatively. In addition, a phase diagram is constructed to illustrate three possible phases, namely, extinction of total population, survival of susceptible rodents and extinction of infected rodents, and survival of the total population. In Sec. IV, we show how the critical sizes and the phase diagram are influenced by the environmental bias and social nature of rodents separately. Analytical expressions for the shift of the critical sizes are derived with a perturbative scheme.

II. POPULATION MODEL FOR HANTAVIRUS INFECTION

A principal model describing hantavirus infection with rodents was proposed by Abramson and Kenkre [8], in which key facts are considered, such as mice being born free from infection and the hantavirus not affecting the behavior of mice. As the hantavirus spreads among rodents, the population of mice is divided into two subpopulations, namely, the population of susceptible mice and the population of infected mice, respectively. The dynamical equations of the population densities for these two subpopulations in one dimension are

$$\begin{aligned}\frac{\partial M_S}{\partial t} &= D \frac{\partial^2 M_S}{\partial X^2} + bM - cM_S - aM_S M_I - \frac{M_S M}{K}, \\ \frac{\partial M_I}{\partial t} &= D \frac{\partial^2 M_I}{\partial X^2} - cM_I + aM_S M_I - \frac{M_I M}{K},\end{aligned}\quad (1)$$

where M_S and M_I are population densities of susceptible mice and infected mice, respectively. b and c represent the birth rate and the death rate of mice. Note that the reproduction rates of infected and susceptible mice are the same since the hantavirus does not have an effect on rodents. The same applies to the death rates for infected and susceptible mice. However, the hantavirus does not transmit from mothers to offspring [6,7], therefore, all newborns are susceptible which breaks the symmetry of the birth term in these equations. The parameter

a characterizes the probability of hantavirus transmission as susceptible mice encounter infected mice. Furthermore, K is the carrying capacity and M is the total population density of mice, $M = M_S + M_I$. The spatial movement of mice is assumed to be microscopically random, which leads to a diffusion term at the macroscopic level. The mobility of mice is characterized by the diffusion coefficient D which is assumed to be the same for both populations.

The evolution of the infected population density is coupled to the susceptible population density, and vice versa. This complexity is readily reduced by identifying the fact that the total population density is $M = M_S + M_I$, and adding up equations listed in Eq. (1), which gives the dynamics of the total population density,

$$\frac{\partial M}{\partial t} = D \frac{\partial^2 M}{\partial X^2} + (b - c)M - \frac{M^2}{K}. \quad (2)$$

It recovers the Fisher equation and is independent of individual subpopulation density. The total population density of mice is therefore determined independently as time progresses, and the evolution of M_I can then be solved accordingly. The dimensionless forms of evolution equations for infected population density and total population density are obtained by the following substitutions: $\tau = (b - c)t$, $x = [D/(b - c)]^{-1/2}X$, $\alpha = aK$, $\beta = c/(b - c)$, $m = M/[(b - c)K]$, $m_i = M_I/[(b - c)K]$. The dimensionless dynamical equations are

$$\begin{aligned}\frac{\partial m}{\partial \tau} &= \frac{\partial^2 m}{\partial x^2} + m - m^2, \\ \frac{\partial m_i}{\partial \tau} &= \frac{\partial^2 m_i}{\partial x^2} + [(\alpha - 1)m - \beta]m_i - \alpha m_i^2,\end{aligned}\quad (3)$$

where m and m_i are dimensionless total population density and infected population density, respectively. Using this model, Abramson and Kenkre showed a close relationship between the temporal evolution of the infected population density and a time-dependent carrying capacity (due to season changes or rainfalls), and discussed the effect of spatial inhomogeneity in carrying capacity (due to the nature of landscapes) on the population density of infected mice. In this paper, we investigate how the spatial confinement could lead to extinction of hantavirus-infected mice while letting uninfected mice thrive, and we extend our discussions to include the nature of sociality of mice as well as environmental asymmetry.

III. CONFINEMENT EFFECTS ON HANTAVIRUS INFECTION

As shown by Kierstead, Slobodkin, and Skellam, there exists a lower bound of the system size (i.e., the critical domain size) for populations to survive when surrounded by a deadly environment. Therefore, it is of interest to investigate the confinement effect in the case of the hantavirus infection. For simplicity, an infinite mortality rate is assumed for mice moving out of the shelter, which reduces the problem to a Dirichlet boundary-value problem. The shelter is set to extend from $x = 0$ to $x = L$, and the population density of mice is zero at the boundary. To determine the critical sizes for the total population and the infected population, the Galerkin truncation method is employed so that coupled PDEs shown

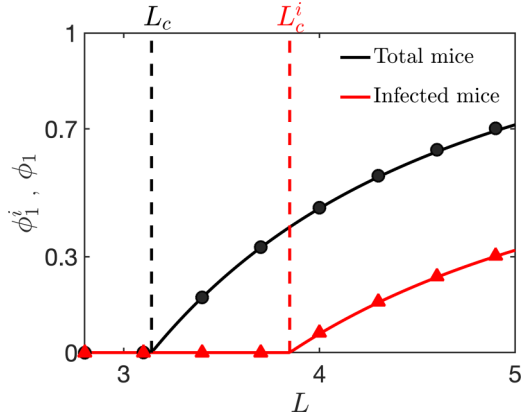


FIG. 1. Bifurcation diagram of the steady state of the principal modes obtained for $\alpha = 6$ and $\beta = 1$. Solid lines are analytical solutions of Eq. (5), and the amplitudes of the principal modes obtained from simulation results of Eq. (3) are shown in symbols. The bifurcation lengths for the total population and the infected population are L_c and L_c^i , respectively. The shelter size gap is defined as the region between L_c and L_c^i , within which the infected population becomes extinct while only the susceptible population survives.

in Eq. (3) are readily reduced to a set of coupled ODEs. Owing to the boundary condition, the total population density and the infected population density are expanded in an infinite series of sinusoidal functions,

$$\begin{aligned}
 m(x, \tau) &= \sum_{k=1}^{\infty} \phi_k(\tau) \sin\left(\frac{k\pi x}{L}\right), \\
 m_i(x, \tau) &= \sum_{k=1}^{\infty} \phi_k^i(\tau) \sin\left(\frac{k\pi x}{L}\right).
 \end{aligned}
 \tag{4}$$

Substituting Eq. (4) into Eq. (3), the evolution equations of $\phi_k(\tau)$ and $\phi_k^i(\tau)$ can be obtained readily by multiplying both sides of Eq. (3) by $\sin(k\pi x/L)$ and integrating it from $x = 0$ to $x = L$. As the domain size is lowered to be close to the critical value, the dominant mode is the principal mode while other modes are negligible. Therefore, after truncating higher-order terms, we obtain

$$\begin{aligned}
 \frac{d\phi_1}{d\tau} &= \left[1 - \left(\frac{\pi}{L}\right)^2\right]\phi_1 - \frac{8}{3\pi}\phi_1^2, \\
 \frac{d\phi_1^i}{d\tau} &= \left[\frac{8(\alpha - 1)}{3\pi}\phi_1 - \beta - \left(\frac{\pi}{L}\right)^2\right]\phi_1^i - \frac{8\alpha}{3\pi}(\phi_1^i)^2,
 \end{aligned}
 \tag{5}$$

which leads to the following nontrivial steady-state solutions:

$$\begin{aligned}
 \phi_1 &= \frac{3\pi}{8} \left[1 - \left(\frac{\pi}{L}\right)^2\right], \\
 \phi_1^i &= \frac{3\pi}{8\alpha} \left[\frac{8(\alpha - 1)}{3\pi}\phi_1 - \beta - \left(\frac{\pi}{L}\right)^2\right].
 \end{aligned}
 \tag{6}$$

The dependence of the steady-state solutions on the domain size is plotted in Fig. 1. The analytical results are in good agreement with numerical simulations of Eq. (3). The simulations are carried out using a finite element method with boundary values set to 0, and a relaxation dynamics to bring the system to the steady state. ϕ_1 and ϕ_1^i are readily obtained

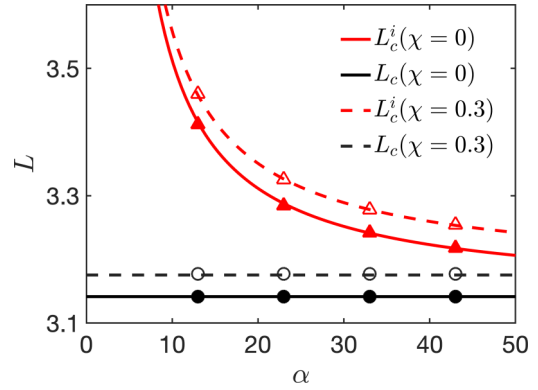


FIG. 2. Phase diagram of extinction of the susceptible population and the infected population with and without the environmental asymmetry. And β is set to be 1. Lines represent solutions of analytical equations shown in Eq. (8), and symbols represent simulation results of Eq. (3) with and without environmental asymmetry. Below the horizontal solid line, both susceptible and infected populations become extinct. In the region enclosed by the solid and the dashed lines, only the susceptible population survives and the infected population becomes extinct. Above the dashed line, both populations survives. The phase boundaries shift as the environmental asymmetry is introduced. And the shelter size gap shrinks as α increases since a high transmission rate and a dense population make it more difficult to eliminate the infected population.

by a discrete sine transform of the simulated steady state. It is clear that the total population would become extinct ($\phi_1 = 0$) as L reduces to π (i.e., $L_c = \pi$). Similarly, by requesting $\phi_1^i(L_c^i) = 0$, we obtain the critical domain size for infected mice:

$$L_c^i = \pi \sqrt{\frac{\alpha}{\alpha - \beta - 1}}.
 \tag{7}$$

It is interesting to note that the critical domain sizes for the total population and the infected population are different, which suggests three possible scenarios for mice populations confined within a shelter of size L surrounded by a harsh environment. If the shelter size is larger than L_c^i , both susceptible and infected mice would survive and coexist. If the size of the shelter is in between L_c^i and L_c , the hantavirus-infected mice become extinct while only susceptible mice survive. And mice would go extinct if the shelter size is smaller than L_c . The critical domain sizes for the total population and the infected population against α are plotted in Fig. 2. A decreased value of α includes a combination of either a smaller infection rate or a smaller carrying capacity, which would reduce the population of infected mice that makes it vulnerable to extinction. As a result, the infected mice requires a larger domain to support its population, and thus a larger L_c^i is obtained while L_c is kept constant. On the other hand, the difference between L_c^i and L_c lessens for large values of α , since the hantavirus can easily be transmitted to susceptible mice. Furthermore, from Eq. (7), the critical domain size for infected mice exists only if $\alpha - \beta - 1 > 0$. This criterion gives rise to a threshold of the carrying capacity $K_c = b/[a(b - c)]$ below which infected mice would become extinct, which is consistent with results obtained by Abramson *et al.* [8].

IV. EFFECTS DUE TO ENVIRONMENTAL ASYMMETRY AND SOCIALITY

A. Environmental bias

The spatial spread of populations density shown in Eq. (1) is spatially isotropic and neglects intraspecies interactions for simplicity, which is plausible for species living in a flat landscape. However, for deer mice, which are widely distributed in North America, their habitat is found to be along the slope of mountains [42–46] where the environmental symmetry is broken due to the varying altitude along the slope. To investigate the effect due to the asymmetry in landscapes, we modify the diffusion terms in Eq. (3) with an additional biased diffusion term. That is to substitute $\frac{\partial^2 m}{\partial^2 x}$ and $\frac{\partial^2 m_i}{\partial^2 x}$ in Eq. (3) by $\frac{\partial}{\partial x}[(\chi + \frac{\partial}{\partial x})m]$ and $\frac{\partial}{\partial x}[(\chi + \frac{\partial}{\partial x})m_i]$, respectively; χ represents the strength of environmental bias, and it is assumed to be the same for infected mice and susceptible mice since the hantavirus does not affect the behavior of mice. Positive and negative values of χ represent biased tendency of mice moving toward $-x$ and $+x$ directions, respectively, since the biased flux is associated with $-\chi m$ for the total population and $-\chi m_i$ for the infected population. Similarly, the GTM is employed to reduce the coupled PDEs to a set of coupled ODEs. However, with the additional biased term, the spatial symmetry is broken and asymmetric population density profiles are expected. Therefore, not only the evolutions of the principal modes [i.e., $\phi_1 \sin(\pi x/L)$ and $\phi_1^i \sin(\pi x/L)$] are important, but also the evolutions of the second modes [i.e., $\phi_2 \sin(2\pi x/L)$ and $\phi_2^i \sin(2\pi x/L)$] have to be considered. One obtains

$$\begin{aligned} \frac{d\phi_1}{d\tau} &= \left[1 - \left(\frac{\pi}{L}\right)^2\right] \phi_1 - \frac{8}{3\pi} \phi_1^2 - \frac{8\chi}{3L} \phi_2 - \frac{32}{15\pi} \phi_2^2, \\ \frac{d\phi_2}{d\tau} &= \left[1 - \left(\frac{2\pi}{L}\right)^2\right] \phi_2 + \frac{8\chi}{3L} \phi_1 - \frac{64}{15\pi} \phi_1 \phi_2, \\ \frac{d\phi_1^i}{d\tau} &= \left[\frac{8(\alpha-1)}{3\pi} \phi_1 - \beta - \left(\frac{\pi}{L}\right)^2\right] \phi_1^i - \frac{8\alpha}{3\pi} (\phi_1^i)^2 \\ &\quad - \frac{8\chi}{3L} \phi_2^i + \frac{32(\alpha-1)}{15\pi} \phi_2 \phi_2^i - \frac{32\alpha}{15\pi} (\phi_2^i)^2, \\ \frac{d\phi_2^i}{d\tau} &= \left[-\beta - \left(\frac{2\pi}{L}\right)^2 + \frac{32(\alpha-1)}{15\pi} \phi_1\right] \phi_2^i + \frac{8\chi}{3L} \phi_1^i \\ &\quad + \frac{32(\alpha-1)}{15\pi} \phi_2 \phi_1^i - \frac{64\alpha}{15\pi} \phi_1^i \phi_2^i. \end{aligned} \quad (8)$$

The critical domain sizes of total population and infected population subject to different degrees of environmental biases are plotted against various values of α in Fig. 2. As shown in Fig. 2, both L_c and L_c^i increase, for the parameters specified, as the spatial symmetry is broken ($\chi \neq 0$). It is clear that terms associated with χ in Eq. (8) have negative impacts on ϕ_1 and ϕ_1^i which reduce populations. This negative effect on populations results from an overall keener competition once the population density profiles become asymmetric due to a nonvanishing χ (that is, one expects a larger value of the integration of m^2 or m_i^2 over space if the bias is present). Therefore, a larger shelter size is required for the species to

survive. However, for other choices of parameters, L_c^i could decrease while L_c always increases with χ .

The quantitative dependence of critical sizes on the environmental bias is obtained by solving steady states of Eq. (8). By requiring $\dot{\phi}_2 = 0$, one obtains

$$\phi_2 = \frac{8\chi\phi_1}{3L} \left[1 - \left(\frac{2\pi}{L}\right)^2 - \frac{64}{15\pi}\phi_1\right]^{-1}, \quad (9)$$

which shows a linear dependence of ϕ_2 on χ , hence, the asymmetry vanishes when $\chi = 0$ as expected. Substitute Eq. (9) into the dynamical equation for ϕ_1 and require $\dot{\phi}_1 = 0$, one obtains an analytical relation between ϕ_1 , L , and χ . For small values of χ , an approximated expression for ϕ_1 is obtained using a perturbation method,

$$\phi_1 \simeq \frac{3\pi}{8} \left[1 - \left(\frac{\pi}{L}\right)^2\right] - \frac{40\pi}{27L^2} \frac{7 + 8(\pi/L)^2}{[1 + 4(\pi/L)^2]^2} \chi^2. \quad (10)$$

To determine the change in the critical domain size of the total population due to χ , we further expand L around the critical size for which the spatial asymmetry is absent, $L = L_c^0 + \delta L$, and substitute it into Eq. (10); note that $L_c^0 = \pi$. The critical size is then determined as ϕ_1 decreases to zero, we obtain $\delta L_c = (32/27\pi^2)L_c^0 \chi^2$. Similarly, we solve the change in the critical size for the infected population,

$$\begin{aligned} \delta L_c^i &= \frac{160}{27\pi^2} \frac{\alpha[5\alpha^2(\beta' + 15) - \alpha\beta'(8\beta' + 125) + 56\beta'^2]}{(4\beta' - 5\alpha)^2[\alpha(\beta' + 15) - 16\beta']} \\ &\quad \times L_c^{i0} \chi^2, \end{aligned} \quad (11)$$

where $\beta' \equiv \beta + 1$ and L_c^{i0} is the critical domain size for the infected population when the environmental bias is absent, see Eq. (7). Therefore, it is expected that the hantavirus-free shelter size gap, within which the infected population becomes extinct while only the susceptible population survives, changes with χ . This shelter size gap is simply $\Delta L_c(\chi) = (L_c^0 - L_c^i) + (\delta L_c^i - \delta L_c)$, and the fractional change in the shelter size gap is $\delta \bar{L} \equiv (\delta L_c^i - \delta L_c)/\Delta L_c(0)$, see Fig. 3. To see whether the environmental bias increases or decreases the shelter size gap for the population confined by a hazard environment, Fig. 4 plots the prefactor σ , defined as $\delta \bar{L} = \sigma \chi^2$, for various values of α and β while L_c^0 and L_c^{i0} are held fixed. It is shown that the shelter size gap could either shrink or expand as the environmental bias is introduced. For systems with a smaller shelter size gap at $\chi = 0$, the fractional change in the shelter size gap is expanded as the environmental bias is present, see Fig. 3. However, the shelter size gap could shrink for systems with a larger L_c^{i0} , in particular, as α gets larger. It is intuitive since a larger value of α corresponds to a larger transmission rate and a larger death rate which reduces the susceptible population and promotes the infected population. As a result, the shelter size gap monotonically decreases with α as shown in Fig. 4.

B. Intraspecies interaction

Apart from the environmental bias, the social nature of animals also has an impact on their movement preference. Rodents are highly social animals, which means there exists

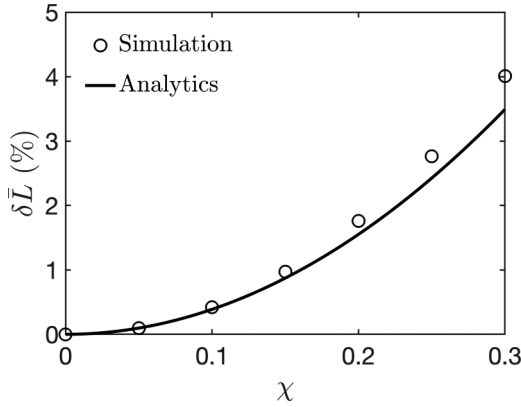


FIG. 3. The fractional change in the shelter size gap, $\delta \bar{L}$, with respect to the biased strength, χ . Here, $\alpha = 6$ and $\beta = 1$ are considered. The solid line is the analytical solution obtained using a perturbation method, and circles are simulations results of Eq. (3) with environmental bias. A quadratic relation is expected since the system is invariant through the following transformation: $\chi \rightarrow -\chi$ and $x \rightarrow -x$.

a non-negligible intraspecies attractive interaction [47]. Intuitively, the sociality of rodents would lead to a more serious infectious state which makes it more difficult to eliminate the hantavirus. For simplicity, if one treats rodents as weakly interacting Brownian particles, through the framework of the nonlinear Fokker-Planck equation introduced in Refs. [48,49], the spatial spread of rodents can be described by additional nonlinear diffusion terms. Take the susceptible population for example, two nonlinear diffusion terms, namely, $\frac{\partial}{\partial x}(M_S \frac{\partial M_S}{\partial x})$ and $\frac{\partial}{\partial x}(M_S \frac{\partial M_I}{\partial x})$, are required in Eq. (1) to describe the social nature of rodents. The physical interpretation of these terms is that the susceptible population is driven by spatial gradients of M_S and M_I due to sociality, and the flux also depends on the local population of susceptible rodents. Similarly, the evolution equation of the infected population density is modified accordingly with two additional terms, namely, $\frac{\partial}{\partial x}(M_I \frac{\partial M_S}{\partial x})$ and $\frac{\partial}{\partial x}(M_I \frac{\partial M_I}{\partial x})$. Therefore, two additional terms,

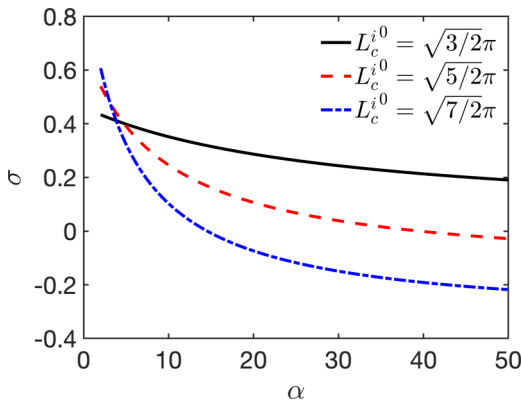


FIG. 4. The value of σ , which characterizes whether the fractional change of the shelter size gap increases or decreases, is plotted as a function of α for different values of L_c^{i0} . The value of σ is shown to decrease monotonically as α increases, since a larger value of α promotes the spread of the hantavirus.

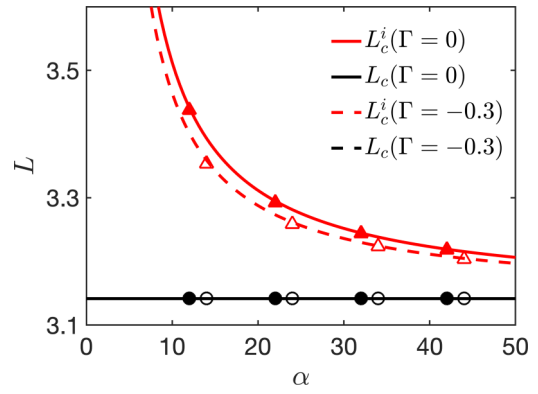


FIG. 5. Phase diagram of extinction of the susceptible population and the infected population for $\beta = 1$ and different degree of sociality. Lines and symbols represent solutions of Eq. (12) and numerical simulations of Eq. (3) with intraspecies interactions, respectively. The solid line (that is L_c) is shown to be independent of Γ , while the dashed line (that is L_c^i) is lower as the social nature intensifies.

namely, $\frac{\partial}{\partial x}(\Gamma m \frac{\partial m}{\partial x})$ and $\frac{\partial}{\partial x}(\Gamma m_i \frac{\partial m_i}{\partial x})$, are required for the evolution equations of m and m_i shown in Eq. (3), respectively. The parameter Γ characterizes the interaction between rodents. Since the additional flux induced by the intraspecies interaction for the total population is associated with $-\Gamma m(\partial m/\partial x)$, the population tends to get away from (move toward) crowded regions if $\Gamma > 0$ ($\Gamma < 0$). Therefore, the value of Γ is taken to be negative in the following discussion. In Fig. 5, numerical simulations show that the critical domain size for the total population remains the same while the critical domain size for the infected population shrinks as sociality is introduced. And the shelter size gap shrinks as the transmission rate increases. Unlike the case considering the environmental bias, the modified diffusion terms here preserve the spatial symmetry with respect to the center of the shelter; thus, harmonics in the population expansion with odd symmetry with respect to the center of the shelter must vanish, and let us take only the first harmonic with even symmetry into consideration for simplicity. By employing the GTM, one obtains

$$\begin{aligned} \frac{d\phi_1}{d\tau} &= \left[1 - \left(\frac{\pi}{L}\right)^2 \right] \phi_1 - \left[\frac{8}{3\pi} + \frac{4\pi\Gamma}{3L^2} \right] \phi_1^2, \\ \frac{d\phi_1^i}{d\tau} &= \left[-\left(\frac{\pi}{L}\right)^2 - \beta + \left(\frac{8(\alpha-1)}{3\pi} - \frac{4\pi\Gamma}{3L^2} \right) \phi_1 \right] \phi_1^i \\ &\quad - \frac{8\alpha}{3\pi} (\phi_1^i)^2. \end{aligned} \tag{12}$$

Once again, since the evolution of the total population is independent of the infected population, the steady state of ϕ_1 is readily obtained when the values of L and Γ are specified. And since the critical domain size is determined by the linear term, the critical domain size of the total population remains to be π regardless of the value of Γ . Similarly, the steady state of ϕ_1^i is obtained by requesting $\phi_1^i = 0$, and the critical domain size of the infected population is obtained approximately by treating Γ as a perturbation parameter. One gets

$$L_c^i(\Gamma) = L_c^{i0} + \frac{\Gamma}{4L_c^{i0}}(L_c^{i0} + L_c^0)(L_c^{i0} - L_c^0), \tag{13}$$

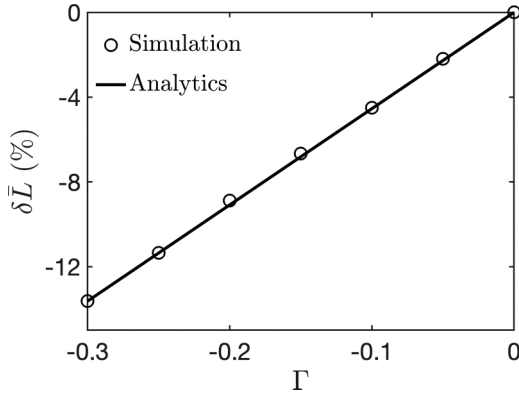


FIG. 6. Variation of $\delta\bar{L}$ with respect to the interacting strength Γ . The parameters are set to be $(\alpha, \beta) = (6, 1)$. The simulation results (circles) of Eq. (3) with intraspecies interactions are in good agreement with analytical result (solid line) obtained using a perturbation method.

and the fractional change in the shelter size gap is

$$\delta\bar{L} \equiv \frac{\delta L_c^i(\Gamma) - \delta L_c(\Gamma)}{L_c^i(0) - L_c(0)} = \frac{\Gamma}{4} \left(1 + \frac{L_c^0}{L_c^i} \right). \quad (14)$$

Note that the nonlinear diffusion term $\frac{\partial}{\partial x}(\Gamma m \frac{\partial m}{\partial x})$ for the total population is negligible as the total population is close to extinction, thus $L_c(\Gamma) = L_c(0) = \pi$, which is independent of Γ . However, for the infected population, the nonlinear diffusion term $\frac{\partial}{\partial x}(\Gamma m_i \frac{\partial m_i}{\partial x})$ is of the same order of m_i as the infected population is close to extinction, hence, L_c^i is reduced as Γ is introduced. Therefore, it is clear that sociality of rodents makes it more difficult to eliminate the hantavirus because the rodents have the tendency to gather together, which increases the chance for hantavirus transmission. It shows consistent and intuitive results that the shelter size gap shrinks more rapidly for larger values of α , as seen in Fig. 5, since higher transmission rates promote the spread of the hantavirus. Figure 6 plots the fractional change of the shelter size gap as a function of Γ which is in good quantitative agreement with Eq. (14). The constant slope of the function $\delta\bar{L}(\Gamma)$ can be expressed in terms of α and β , one gets $\delta\bar{L}/\Gamma = [1 + \sqrt{(\alpha - \beta - 1)/\alpha}]/4$.

V. SUMMARY AND DISCUSSIONS

In this paper, we investigate the extinction criterion for rodents infected with the hantavirus surrounded by a hazard environment analytically and numerically. Owing to the fact that the hantavirus does not transmit from mothers to newborn mice, which breaks the symmetry between susceptible and infected population, the requirement of the minimum domain size in order for mice to survive (that is, the KiSS size) is different. We show that this asymmetry gives rise to the possibility of eliminating the infected population while letting the susceptible population thrive as one confines rodents in a shelter of certain size. It preserves the integrity of the food web while eradicating the infectious disease. The shelter size gap, within which the infected population becomes extinct while only the susceptible population survives, is shown analytically to depend closely on the transmission rate, the carrying capac-

ity, and the birth and death rate of rodents. The shelter size gap broadens if the transmission rate or the carrying capacity is low, since both reduce the increase in the rate of infected population.

In addition, two common factors observed in nature, namely, environmental bias and intraspecies interaction, that influence the spatial movement of rodents are introduced to see how these affect the shelter size gap. The impact of the existence of the environmental bias such as a tilted landscape on the critical domain sizes is the following: It creates an asymmetric spatial population distribution that results in an overall keener competition for the total population which increases its critical domain size. However, for the infected population, the critical domain size could increase due to keener competition caused by the spatial asymmetry, but the critical domain size could decrease as well since more densely populated region due to the spatial asymmetry promotes the spread of the hantavirus. As to the social nature of rodents, the critical domain size is shown to be invariant for the total population since the effect of sociality is negligible because the total population is near extinction. And the critical domain size for the infected population decreases since the population flux of the infected population driven by the sociality is coupled to the spatial gradient of the total population which is still pronounced as the infected population is near extinction. The shelter size gap then decreases as the social nature intensifies, which is intuitive, since sociality drives the population to be more localized that favors the spread of the hantavirus.

The present theory, although in one dimension, is applicable to rodents in a two-dimensional stripe area where the aspect ratio of the domain is sufficiently large. Since the spatial variation of the population along the extended dimension is negligible over the length scale of the shorter dimension, the population can be treated as homogeneous along the extended dimension. Therefore, our theory simply describes the population dynamics along the shorter dimension. To examine the validity of the proposed strategy, we estimate the parameters of rodent population and the hantavirus transmission with field data reported in Ref. [7]. The birth rate b and the death rate c are obtained by the reported exponential-like growth from a small population over a few months and the reported longevity of deer mice; one gets approximately $b \simeq 20$ per year and $c \simeq 4$ per year. Using the incidence rate and the number of infected and susceptible rodents being captured, the transmission coefficient a is estimated to be $0.02/\mathcal{A}$ per mouse per year for a trapping area \mathcal{A} if a 10% capture rate is assumed. By assuming a saturated total population to be on the order of thousands during outbreaks, the carrying capacity $K\mathcal{A}$ is estimated to be on the order of hundreds mice-year. With these parameters estimated from the field research, we readily obtain key dimensionless parameters used in the paper: $\alpha = 2$ and $\beta \equiv c/(b - c) \simeq 0.25$. The dimensionless critical domain size for infected mice is then 1.6π , while the dimensionless critical domain size for susceptible mice is π . The physical length dimension can be restored once we know the mobility of rodents. D is reported to be about 500 m^2 per day for deer mice [50]. Therefore, the critical domain size for the susceptible mice is about 335.5 m , and the critical domain size for the infected mice is about 547.9 m . The uncertainty of the shelter sizes can be

estimated as we assume a 10% error in the parameters. That is, according to our theoretical work, if one confines the rodent population within a stripe region surrounded by a deadly environment with the shorter dimension between 335.5 ± 27.2 m and 547.9 ± 78.3 m, the infected population would become extinct.

It is worth noting that, although the continuum approach employed here sheds light on the confinement effects on the extinction condition, the framework of the model is not applicable when the rodent population is sparse. It is of interest to employ discrete models that consider fluctuation in population [51,52], and probabilistic migration and interaction [53] to

examine the critical size. It has been shown that the stochasticity is crucial in predicting the critical size. Nevertheless, the analytical results obtained from the continuum model serves as a guideline for the critical size.

ACKNOWLEDGMENTS

The authors gratefully acknowledge the support of the Ministry of Science and Technology, Taiwan (Grants No. MOST 109-2112-M-007-005- and No. MOST 110-2112-M-007-003-), and the support from the National Center for Theoretical Sciences, Taiwan.

-
- [1] C. Schmaljohn and B. Hjelle, *Emerging Infect. Dis.* **3**, 95 (1997).
- [2] T. L. Yates, J. N. Mills, C. A. Parmenter, T. G. Ksiazek, R. R. Parmenter, J. R. Vande Castle, C. H. Calisher, S. T. Nichol, K. D. Abbott, J. C. Young, M. L. Morrison, B. J. Beaty, J. L. Dunnun, R. J. Baker, J. Salazar-Bravo, and C. J. Peters, *Bioscience* **52**, 989 (2002).
- [3] S. T. Nichol, C. F. Spiropoulou, S. Morzunov, P. E. Rollin, T. G. Ksiazek, H. Feldmann, A. Sanchez, J. Childs, S. Zaki, and C. J. Peters, *Science* **262**, 914 (1993).
- [4] J. E. Childs, T. G. Ksiazek, C. F. Spiropoulou, J. W. Krebs, S. Morzunov, G. O. Maupin, K. L. Gage, P. E. Rollin, J. Sarisky, R. E. Enscore, J. K. Frey, C. J. Peters, and S. T. Nichol, *J. Infect. Dis.* **169**, 1271 (1994).
- [5] G. E. Glass, J. E. Childs, G. W. Korch, and J. W. LeDuc, *Epidemiol. Infect.* **101**, 459 (1988).
- [6] J. N. Mills, T. G. Ksiazek, C. J. Peters, and J. E. Childs, *Emerging Infect. Dis.* **5**, 135 (1999).
- [7] C. H. Calisher, W. Sweeney, J. N. Mills, and B. J. Beaty, *Emerging Infect. Dis.* **5**, 126 (1999).
- [8] G. Abramson and V. M. Kenkre, *Phys. Rev. E* **66**, 011912 (2002).
- [9] G. Abramson, V. M. Kenkre, T. L. Yates, and R. R. Parmenter, *Bull. Math. Biol.* **65**, 519 (2003).
- [10] J. Buceta, C. Escudero, F. J. de la Rubia, and K. Lindenberg, *Phys. Rev. E* **69**, 021906 (2004).
- [11] N. Kumar, R. R. Parmenter, and V. M. Kenkre, *Phys. Rev. E* **82**, 011920 (2010).
- [12] B. Hjelle and G. E. Glass, *J. Infect. Dis.* **181**, 1569 (2000).
- [13] W. C. Allee, *Animal Aggregations, a Study in General Sociology* (The University of Chicago Press, Chicago, 1931), p. 452.
- [14] P. A. Stephens, W. J. Sutherland, and R. P. Freckleton, *Oikos* **87**, 185 (1999).
- [15] D. W. Morris, *Ecology* **83**, 14 (2002).
- [16] A. M. Kramer, B. Dennis, A. M. Liebhold, and J. M. Drake, *Popul. Ecol.* **51**, 341 (2009).
- [17] N. Kumar, M. N. Kuperman, and V. M. Kenkre, *Phys. Rev. E* **79**, 041902 (2009).
- [18] G. Abramson, L. Giuggioli, R. R. Parmenter, and V. M. Kenkre, *J. Theor. Biol.* **319**, 96 (2013).
- [19] V. Kenkre, *Phys. A (Amsterdam, Neth.)* **356**, 121 (2005).
- [20] V. M. Kenkre, L. Giuggioli, G. Abramson, and G. Camelo-Neto, *Eur. Phys. J. B* **55**, 461 (2007).
- [21] J. A. Reinoso and F. J. de la Rubia, *Phys. Rev. E* **87**, 042706 (2013).
- [22] J. A. Reinoso and F. J. de la Rubia, *Phys. Rev. E* **91**, 032703 (2015).
- [23] J. G. Skellam, *Biometrika* **38**, 196 (1951).
- [24] H. Kierstead and L. Slobodkin, *J. Mar. Res.* **12**, 141 (1953).
- [25] A. Okubo, *Diffusion and Ecological Problems: Mathematical Models* (Springer-Verlag, New York, 1980).
- [26] S. Harris, *Phys. Rev. E* **62**, 4032 (2000).
- [27] O. Vasilyeva and F. Lutscher, *Can. Appl. Math. Q.* **18**, 439 (2010).
- [28] V. Mendez and D. Campos, *Phys. Rev. E* **77**, 022901 (2008).
- [29] N. Kumar and V. Kenkre, *Phys. A (Amsterdam, Neth.)* **390**, 257 (2011).
- [30] D. J. Pamplona da Silva and R. Kraenkel, *Phys. A (Amsterdam, Neth.)* **391**, 142 (2012).
- [31] K. A. Dahmen, D. R. Nelson, and N. M. Shnerb, *Statistical Mechanics of Biocomplexity* (Springer, Berlin, Heidelberg, 1999), pp. 124–151.
- [32] K. Dahmen, D. Nelson, and N. Shnerb, *J. Math. Biol.* **41**, 1 (2000).
- [33] T. Neicu, A. Pradhan, D. A. Larochelle, and A. Kudrolli, *Phys. Rev. E* **62**, 1059 (2000).
- [34] V. M. Kenkre and M. N. Kuperman, *Phys. Rev. E* **67**, 051921 (2003).
- [35] N. Perry, *J. R. Soc. Interface* **2**, 379 (2005).
- [36] V. M. Kenkre and N. Kumar, *Proc. Natl. Acad. Sci. USA* **105**, 18752 (2008).
- [37] J. Huisman, M. Arrayás, U. Ebert, B. Sommeijer, and A. E. J. Elser, *Am. Nat.* **159**, 245 (2002).
- [38] P. Stouffer, R. Bierregaard, C. Strong, and T. Lovejoy, *Conserv. Biol.* **20**, 1212 (2006).
- [39] G. Ferraz, J. D. Nichols, J. E. Hines, P. C. Stouffer, R. O. Bierregaard, and T. E. Lovejoy, *Science* **315**, 238 (2007).
- [40] W. Artilles, P. G. S. Carvalho, and R. A. Kraenkel, *J. Math. Biol.* **57**, 521 (2008).
- [41] B. Galerkin, *Vestnik Inzh* **19**, 897 (1915).
- [42] J. O. Wolff and B. Hurlbutt, *J. Mammal.* **63**, 666 (1982).
- [43] C. D. Stah, *J. Mammal.* **61**, 141 (1980).
- [44] R. E. Barry, M. A. Botje, and L. B. Grantham, *J. Mammal.* **65**, 145 (1984).
- [45] S. G. Parren and D. E. Capen, *J. Mammal.* **66**, 36 (1985).

- [46] G. B. Sekgororoane and T. G. Dilworth, *Can. J. Zool.* **73**, 1432 (1995).
- [47] N. S. Lee, A. K. Beery, and D. R. Grattan, *Neuroendocrine Regulation of Behavior* (Springer International Publishing, Cham, 2019), pp. 211–238.
- [48] S. Savel'ev, F. Marchesoni, and F. Nori, *Phys. Rev. Lett.* **91**, 010601 (2003).
- [49] S. Savel'ev, F. Marchesoni, A. Taloni, and F. Nori, *Phys. Rev. E* **74**, 021119 (2006).
- [50] G. Abramson, L. Giuggioli, V. Kenkre, J. Drago, R. Parmenter, C. Parmenter, and T. Yates, *Ecol. Complexity* **3**, 64 (2006).
- [51] V. Méndez, I. Llopis, D. Campos, and W. Horsthemke, *Theor. Popul. Biol.* **77**, 250 (2010).
- [52] C. Escudero, J. Buceta, F. J. de la Rubia, and K. Lindenberg, *Phys. Rev. E* **69**, 021908 (2004).
- [53] S. Berti, M. Cencini, D. Vergni, and A. Vulpiani, *Phys. Rev. E* **92**, 012722 (2015).